BIODIVERSITAS
Volume 26, Number 12, December 2025
Pages: 6000-6013

ISSN: 1412-033X
E-ISSN: 2085-4722
DOI: 10.13057/biodiv/d261204

Phytochemical composition and antibacterial potential of *Melastoma malabathricum* against *Staphylococcus aureus* with in silico insights into MRSA target proteins

FEBRIA ELVY SUSANTI[1], MAI EFDI[1,♥], SYAFRIZAYANTI[1], ABDI WIRA SEPTAMA[2], NURYANI TURABBY[1]

[1]Department of Chemistry, Faculty of Mathematics and Natural Sciences, Universitas Andalas. Limau Manis, Padang 25163, West Sumatra, Indonesia. Tel./fax.: +62-751-71671, ♥email: maiefdi@sci.unand.ac.id

[2]Research Center for Pharmaceutical Ingredients and Traditional Medicine, National Research and Innovation Agency. Jl. Raya Jakarta-Bogor Km. 46 Cibinong, Bogor 16911, West Java, Indonesia

Manuscript received: 23 September 2025. Revision accepted: 25 November 2025.

Abstract. *Susanti FE, Efdi M, Syafrizayanti, Septama AW, Turabby N. 2025. Phytochemical composition and antibacterial potential of* Melastoma malabathricum *against* Staphylococcus aureus *with in silico insights into MRSA target proteins. Biodiversitas 26: 6000-6013.* The global rise in antimicrobial resistance highlights the need to explore new antibacterial agents derived from natural sources. *Melastoma malabathricum*, a medicinal plant rich in phenolic compounds, was investigated for its antioxidant and antibacterial properties, with additional in silico analysis of potential interactions with MRSA-related target proteins. Methanol extracts from different plant parts (leaves, stems, fruits, roots, and flowers) were evaluated for their Total Phenolic Content (TPC), antioxidant activity, and antibacterial effects against methicillin-sensitive *Staphylococcus aureus* (MSSA, ATCC 29213) and *Escherichia coli* (ATCC 25922). The flower extract showed the widest inhibition zone of 14.17 mm against *S. aureus* ATCC 29213 (MSSA), and the highest IC_{50} value (89.22 mg/L) was obtained from the root extract, indicating the lowest antioxidant activity. The TPC of the extracts reached 140.84 mg GAE/g. Molecular docking revealed that afzelin, quercetin, and trifolin may bind to MRSA-associated proteins, including PBP2a, DdlB, and FabH, suggesting possible mechanisms underlying the observed antibacterial effects. These findings imply that phenolic compounds in *M. malabathricum* could act through multiple molecular targets, contributing to its biological activities. However, since the antibacterial assays were conducted using a methicillin-sensitive strain, further validation using MRSA isolates is required to confirm the predicted inhibitory potential. Overall, this study provides a preliminary understanding of the phenolic composition and antibacterial potential of *M. malabathricum*, supporting its continued investigation as a natural source of bioactive compounds.

Keywords: Antioxidant activity, bioactive metabolites, LC-HRMS profiling, *Melastoma malabathricum*, MRSA targets

INTRODUCTION

Methicillin-Resistant *Staphylococcus aureus* (MRSA) is a major global health concern due to its resistance to β-lactam antibiotics mediated by the *mecA* gene, which encodes Penicillin-Binding Protein 2a (PBP2a) (Lade and Kim 2023). The rapid emergence and spread of MRSA in both healthcare and community settings have resulted in increased morbidity, mortality, and healthcare costs (Shoaib et al. 2023). Recognized by the World Health Organization (WHO) as a high-priority pathogen, MRSA underscores the urgent need for new antibacterial strategies that extend beyond conventional antibiotics (Lee et al. 2018; Shah et al. 2024).

In response to this challenge, researchers have increasingly explored natural products as alternative sources of antibacterial agents (Chaachouay and Zidane 2024). Medicinal plants remain valuable reservoirs of pharmacologically active molecules, many of which display antibacterial, antifungal, and antioxidant activities (Azizan et al. 2020; Lafraxo et al. 2022). Among them, *Melastoma malabathricum* L. (commonly known as *senduduk*), a plant widely distributed across Southeast Asia, has long been used in traditional medicine to treat skin infections, promote wound healing, and alleviate gastrointestinal and inflammatory conditions. Phytochemical studies have shown that the plant contains flavonoids, phenolic acids, tannins, and triterpenoids, which contribute to its diverse biological effects (Kumar et al. 2021; Zakaria et al. 2022; Hipol et al. 2023). Although some studies have reported antibacterial activity of *M. malabathricum* against *Staphylococcus aureus*, studies providing analyses of its molecular interactions with MRSA resistance-related proteins remain relatively limited (Verma et al. 2022).

Phenolic compounds are known to play a central role in the biological activities of *M. malabathricum* (Zakaria et al. 2022). These compounds possess strong antioxidant capacity by scavenging Reactive Oxygen Species (ROS), thereby preventing oxidative stress and protecting cellular components from damage. Beyond their antioxidant role, phenolics can disrupt bacterial cell membranes, inhibit key enzymes, and induce oxidative stress within bacterial cells, collectively contributing to antibacterial effects (Bouarab-Chibane et al. 2019; Lee et al. 2024). Because of these multitarget actions, phenolic compounds are considered potential candidates for the development of dual-function

agents that can mitigate oxidative stress while limiting bacterial growth.

Oxidative stress has also been linked to bacterial resistance mechanisms and biofilm formation (Vaishampayan and Grohmann 2022). MRSA infections are often associated with elevated oxidative stress, which promotes bacterial survival and persistence (da Cruz Nizer et al. 2024). Therefore, identifying natural compounds that exhibit both antioxidant and antibacterial effects could be beneficial in managing infections and reducing oxidative damage (Tan et al. 2024).

Molecular docking, a computational technique that predicts interactions between small molecules and biological targets, has become an essential tool in drug discovery. It enables the simulation of binding interactions between bioactive compounds and bacterial proteins such as PBP2a, the enzyme responsible for MRSA's resistance to β-lactam antibiotics. When combined with advanced analytical techniques such as Liquid Chromatography, High-Resolution Mass Spectrometry (LC-HRMS), docking analysis can provide valuable insights into the potential molecular mechanisms underlying antibacterial effects (Pisano et al. 2019). The integration of experimental assays and in silico evaluations thus offers a comprehensive framework for understanding antibacterial potential.

While *Melastoma malabathricum* demonstrates diverse pharmacological activities, relatively few studies have adopted a combined phytochemical, biological, and computational approach (Zakaria et al. 2022). Previous work by Alwash et al. (2013) demonstrated that *M. malabathricum* leaves possess antibacterial and antioxidant activities via bio-guided fractionation and flavonoid isolation. In this study, LC-HRMS metabolite profiling, correlation analysis, and in silico docking were employed to examine the phytochemical composition and potential interactions of major phenolic compounds with MRSA-associated proteins, particularly Penicillin-Binding Protein 2a (PBP2a). The phytochemical composition, antioxidant activity, and antibacterial properties of *M. malabathricum* extracts were evaluated using methicillin-sensitive *S. aureus* (MSSA, ATCC 29213) and *E. coli* as test organisms, alongside in silico docking targeting MRSA proteins. These results provide information on the phytochemical composition, antioxidant activity, and predicted interactions with MRSA-associated proteins, which could guide further studies.

MATERIALS AND METHODS

Plant collection

Fresh leaves of *Melastoma malabathricum* were collected from the vicinity of Universitas Andalas, Padang, West Sumatra, Indonesia (0°54'32.58" S, 100°28'51.03" E). The plant specimen was identified by a certified botanist at the Herbarium ANDA, Universitas Andalas. The voucher specimen (ANDA00028186) has been deposited in the Herbarium ANDA and is available for reference upon reasonable request. The collected samples were cleaned, air-dried, ground into powder, and stored for subsequent extraction.

Plant extract preparation

Leaves, stems, roots, flowers, and fruits (100 g) were dried, powdered, and individually extracted with methanol at a 1:10 (w/v) ratio for 72 hours, following the protocols outlined by Zakaria et al. (2022) and Kumar et al. (2023). After maceration, the filtrate was collected, and the residue was re-macerated in methanol. It was repeated three times. The resulting filtrates were concentrated under reduced pressure and stored at 4°C in amber containers until further analysis. The yield was calculated using the following formula:

$$\text{Yield (\%)} = \frac{\text{Weight of extract obtained}}{\text{Dry weight of the plant material}} \times 100$$

Phytochemical screening

A qualitative screening of major phytoconstituents in the methanolic extracts of *M. malabathricum* was carried out using widely accepted phytochemical procedures. Several steps were adjusted to accommodate the use of fresh plant material and to improve clarity during endpoint observation. The methodological modifications were adapted from Ramli et al. (2022), with modifications mainly in sample preparation, phase separation, and color development. The presence of each metabolite group was recorded as (+), whereas its absence was noted as (-).

Sample preparation

Each fresh plant part (4 g) was chopped finely and macerated in methanol. The mixture was heated in a water bath at 40°C for 15 minutes. The filtrate was left to evaporate at room temperature until dry. The dried extract was reconstituted with 5 mL of chloroform and 5 mL of distilled water (1:1), shaken vigorously, and allowed to stand until two distinct layers developed. The aqueous layer was used for the detection of saponins, flavonoids, and phenolic compounds, while the chloroform layer was reserved for the evaluation of triterpenoids and steroids.

Saponins

Two milliliters of the aqueous layer were shaken for 30 seconds, then 2 drops of concentrated HCl were added. A foam that remained after agitation indicated a positive for saponins.

Flavonoids

One milliliter of the aqueous layer was mixed with roughly 50 mg of finely cut magnesium ribbon. Afterward, 2 drops of concentrated HCl were added. The reaction produced a reddish-orange color, consistent with a positive flavonoid test.

Phenolics

One milliliter of the aqueous layer was treated with 2 drops of a 2% ferric chloride solution. The mixture developed a dark bluish-black color, a reaction commonly associated with phenolic compounds.

Triterpenoids and steroids

The chloroform layer (0.3 mL) was placed on porcelain plates and allowed to air-dry, followed by the addition of concentrated H_2SO_4 (50 µL) and acetic anhydride (50 µL) consecutively. The formation of a red color indicated a positive triterpenoid result, while the formation of a green hue indicated a positive steroid result.

Alkaloids

Fresh plant material (4 g) was ground with clean sand, moistened with 1 mL of chloroform, then added with 5 mL of 0.05 M ammoniated chloroform and filtered. The filtrate was shaken with 5 mL of 2 N sulfuric acid to form two layers. The acidic layer was added with Mayer's reagent; the formation of a white, cloudy precipitate indicated a positive result for alkaloids.

Coumarins

Methanolic extracts (5 µL per spot) were applied to silica-gel TLC plates (5 × 10 cm), dried, and eluted using a mobile phase composed of ethyl acetate and hexane (2:8, v/v). After drying, the plates were sprayed with 1% NaOH and viewed under UV light at 365 nm. The emergence of bright blue fluorescence was typically associated with coumarins.

Metabolite profiling

Methanolic extracts were analyzed using LC-HRMS (UHPLC-Orbitrap, Thermo Scientific) to profile the chemical composition. A water-methanol gradient containing 0.1% formic acid was applied to separate metabolites. Compounds were tentatively identified based on accurate mass, retention time, and MS fragmentation patterns using Compound Discoverer® in combination with the MzCloud database (Windarsih et al. 2022). To enhance the reliability of metabolite identification, future studies should include comparisons with authentic standards and MS/MS fragmentation matching. In this study, putative identifications were based on high-resolution mass data and database matches (MzCloud score >80%), providing a preliminary indication of the chemical composition.

Total phenolic content

Total Phenolic Content (TPC) was determined using the Folin-Ciocalteu method (Itam et al. 2021; Lawag et al. 2023) with minor modifications. Gallic acid standards were prepared and diluted to 20-120 mg/L. Plant extracts were dissolved in methanol (500 mg/L), and aliquots were mixed with Folin-Ciocalteu reagent and Na_2CO_3. After 2 hours of incubation and absorbance measurement at 760 nm, results were expressed as mg Gallic Acid Equivalents (GAE)/g extract.

Antioxidant activity

The antioxidant activity of the extracts was evaluated using the DPPH free radical scavenging assay, with minor modifications based on the methods described by Yeo and Shahidi (2019). Stock solutions of ascorbic acid and the plant extracts (1.000 mg/L) were prepared in methanol and diluted to the required concentrations. Each sample or standard (2 mL) was combined with 3 mL of 0.1 mM DPPH solution and incubated in the dark for 30 minutes. Absorbance was recorded at 517 nm, and the percentage of inhibition was calculated using the formula:

$$\% \text{ Inhibition} = \frac{\text{Abs\_control} - \text{Abs\_sample}}{\text{Abs\_control}} \times 100$$

The IC_{50} values were subsequently determined by regression analysis.

Antibacterial assay

Antibacterial activity was assessed using the disc diffusion method with minor modifications from CLSI (2023). Methanolic extracts of the plant (20 µL/disc) were tested against *Staphylococcus aureus* ATCC 29213 (MSSA) and *Escherichia coli* ATCC 25922. Ampicillin (50 µg/disc) and 0.1% DMSO were employed as positive and negative controls, respectively. The diameters of the inhibition zones on Mueller-Hinton agar were recorded after 24 hours of incubation at 37°C.

Molecular docking analysis

The chemical structures of selected metabolites were retrieved from PubChem and prepared using AutoDock Tools 1.5.6, which was used as the graphical interface for AutoDock Vina 1.1.2. Ligand preparation involved removing water molecules, adding polar hydrogens, assigning Kollman charges, and converting the structures to pdbqt format. Protein structures of penicillin-binding protein 2a (PBP2a; PDB ID: 1MWT), D-alanine-D-alanine ligase B (DdlB; PDB ID: 4JCN), and β-ketoacyl-ACP synthase III (FabH; PDB ID: 5M18) were obtained from the Protein Data Bank and processed following standard protocols for docking studies. Docking simulations were performed using AutoDock Vina 1.1.2, a validated molecular docking engine that allows flexible ligand and rigid receptor docking. The exhaustiveness was set to 32, and ten docking poses were generated for each ligand. Grid box parameters were centered on the active sites of the target proteins based on their co-crystallized ligands, with dimensions adjusted to fully encompass the binding pockets: 16 Å (PBP2a), 18 Å (DdlB), and 12 Å (FabH). The slightly larger grid size for DdlB accommodated its extended catalytic site. To ensure docking reliability, RMSD-based redocking of co-crystallized ligands was performed, confirming that the docking parameters reproduced native binding poses within an RMSD threshold of 2.0 Å. Binding affinities (kcal/mol) and molecular interactions, including hydrogen bonds, hydrophobic contacts, and π-π stacking, were analyzed using Discovery Studio Visualizer v25.1.0.24284 and PyMOL 3.1.4.1. The selected target proteins represent key mechanisms associated with MRSA resistance: PBP2a mediates β-lactam resistance, DdlB contributes to peptidoglycan cross-linking, and FabH is involved in fatty acid biosynthesis.

Data analysis

All measurements were performed in triplicate (n = 3) to ensure the reproducibility and reliability of the experimental data. Conducting measurements in triplicate minimizes random errors and allows for accurate calculation of mean values and Standard Deviations (SD). Results are

expressed as Total Phenolic Content (TPC, mg GAE/g), antioxidant activity (IC_{50}, mg/L), and antibacterial activity (inhibition zone diameter, mm). Statistical comparisons among extracts were carried out using One-Way Analysis of Variance (ANOVA) followed by Duncan's post-hoc test to determine significant differences at $p<0.05$. Pearson correlation was used to assess the relationships among TPC, IC_{50}, and inhibition zones. Reproducibility was maintained by performing all experiments under identical laboratory conditions, employing standardized extraction procedures, consistent analytical methods, and properly calibrated instruments. Statistical analyses were conducted using IBM SPSS Statistics version 27, and all results were verified for accuracy and validity.

As detailed in the molecular docking analysis section, docking simulations were conducted using AutoDock Vina version 1.5.6. Docking results were evaluated based on binding affinity (ΔG, kcal/mol) and key interaction types, including hydrogen bonding, hydrophobic contacts, and π-π stacking, using Discovery Studio Visualizer version 25.1.0.24284 and PyMOL version 3.1.4.1. The visualized docking poses were examined to identify critical residues and binding mechanisms contributing to ligand-protein affinity.

RESULTS AND DISCUSSION

Extraction of methanolic extracts

Methanolic extraction of *M. malabathricum* resulted in varying yields among the different plant parts. Flowers and leaves had high yields (6.08% and 5.15%, respectively), suggesting they contain more extractable metabolites. In contrast, roots, stems, and fruits yielded lower amounts, with fruits producing the lowest yield (2.01%). The extraction yields for all plant parts are summarized in Table 1.

Phytochemical screening

Phytochemical screening confirmed the presence of flavonoids and phenolics in all extracts, while the distribution of other metabolite classes varied among plant parts. The complete profiles are provided in Table 2.

LC-HRMS metabolite profiling

LC-HRMS analysis identified 37 metabolites from *M. malabathricum*, representing flavonoids, phenolics, fatty acids, terpenoids, alkaloids, and amino acids. Flavonoids and triterpenoids were the most abundant classes. Key metabolites included quercetin, afzelin, trifolin, and ursolic acid, all known for their antioxidant and antibacterial activities. The the complete list is presented in Table 3.

Total phenolic content

Total Phenolic Content (TPC) varied among the different parts of *M. malabathricum*. The highest TPC was observed in the fruit and leaf extracts, while the flower and root extracts contained lower levels. Stem extracts were not included due to insufficient material. The detailed TPC values are presented in Table 4.

Antioxidant activity

The antioxidant activity of *M. malabathricum* extracts was measured by the DPPH assay and is summarized in Table 5. The root extract demonstrated the highest radical scavenging activity, followed by the flower, leaf, and fruit extracts. Ascorbic acid, used as a positive control, showed the most potent antioxidant activity.

Antibacterial activity

The antibacterial activity of *M. malabathricum* extracts varied among different plant parts, as summarized in Table 6. The flower extract exhibited the strongest inhibition zones, with growth inhibition of 14.17 mm against *S. aureus* (MSSA) and 9.67 mm against *E. coli*. The stem and leaf extracts showed moderate antibacterial activity, while the root extract had the weakest effect. Ampicillin, the positive control, displayed the largest inhibition zones (21.65 mm against *S. aureus* (MSSA) and 21.03 mm against *E. coli*). The negative control (DMSO) showed no inhibition. In summary, inhibition diameters ranged from 5.37 to 14.17 mm for *S. aureus* and 7.23 to 10.57 mm for *E. coli*.

Interrelation between phenolic, antioxidant, and antibacterial activities

A strong negative correlation was observed between Total Phenolic Content (TPC) and antioxidant activity (IC_{50}) ($r = -0.97$, $p = 0.03$). Regression analysis yielded the model $IC_{50} = 126.42 - 0.61 \times TPC$ ($R^2 = 0.93$, $F = 28.05$, $p = 0.03$). Correlations between TPC and antibacterial activities were positive but not statistically significant ($r = 0.30$, $p = 0.70$ for *S. aureus*; $r = 0.84$, $p = 0.16$ for *E. coli*). A negative trend was observed between IC_{50} and the inhibition zone against *E. coli* ($r = -0.94$, $p = 0.06$). The sample size was $n = 4$.

Table 1. Extract yield of *Melastoma malabathricum*

Plant part	Yield (% w/w)
Leaf	5.15±0.78
Stem	2.57±0.75
Root	4.54±0.72
Flower	6.08±1.90
Fruit	2.01±0.78

Note: Yield is expressed as the percentage of extract weight relative to the dry weight of the plant material. Each extraction was performed in triplicate (n = 3). Due to the limited number of replicates, results are presented as mean±SD and interpreted descriptively

Table 2. Phytochemical composition of *M. malabthricum* extracts

Compound	Leaf	Stem	Root	Flower	Fruit
Flavonoids	+	+	+	+	+
Phenolics	+	+	+	+	+
Saponins	-	-	+	+	+
Steroids	+	+	-	+	-
Triterpenoids	-	-	+	-	+
Alkaloids	+	-	+	+	+
Coumarins	+	-	+	+	+

Note: +: Presence, -: Absence

Table 3. LC-HRMS metabolite profiling of *Melastoma malabathricum*

Compound	Molecular formula	Retention time (min)	Molecular weight (da)
Terpenoids			
(1S,4S,5R,10S,13S,17S,19S,20R)-10-hydroxy-4,5,9,9,13,19,20-heptamethyl-24-oxahexacyclo	$C_{30}H_{46}O_3$	12.297	454.34
(3β,5ξ,9ξ)-3,6,19-trihydroxyurs-12-en-28-oic acid	$C_{30}H_{48}O_5$	10.949	488.35
DL-α-Tocopherol	$C_{29}H_{50}O_2$	18.923	430.38
NP-021050	$C_{30}H_{48}O_4$	12.579	472.35
Ursolic acid*	**$C_{30}H_{48}O_3$**	**14.273**	**456.36**
Phenolic			
4-Phenylbutyric acid	$C_{10}H_{12}O_2$	19.289	164.08
Kojic acid	$C_6H_6O_4$	1.238	142.03
Nicotinic acid	$C_6H_5NO_2$	0.971	123.03
Phloroglucinol	$C_6H_6O_3$	2.119	126.03
Flavonoids			
2-(3,4-dihydroxyphenyl)-5,7-dihydroxy-3-{[(2S,3R,4R,5R,6S)-3,4,5-trihydroxy-6-methyloxan-2-yl]oxy}-4H-chromen-4-one	$C_{21}H_{20}O_{11}$	6.340	448.10
2-(3,4-dihydroxyphenyl)-5,7-dihydroxy-3,4-dihydro-2H-1-benzopyran-4-one	$C_{15}H_{12}O_6$	6.468	288.06
Afzelin*	**$C_{21}H_{20}O_{10}$**	**6.769**	**432.10**
Hyperoside	$C_{21}H_{20}O_{12}$	5.643	464.09
Naringenin	$C_{15}H_{12}O_5$	8.344	272.07
Quercetin*	**$C_{15}H_{10}O_7$**	**6.236**	**302.04**
Rutin	$C_{27}H_{30}O_{16}$	5.458	610.15
Taxifolin	$C_{15}H_{12}O_7$	4.787	304.06
Trifolin*	**$C_{21}H_{20}O_{11}$**	**6.014**	**448.10**
Fatty acids			
1-Linoleoyl glycerol	$C_{21}H_{38}O_4$	12.341	354.28
1-Stearoylglycerol	$C_{21}H_{42}O_4$	12.409	358.31
12-Oxo phytodienoic acid	$C_{18}H_{28}O_3$	12.344	292.20
13(S)-HOTrE	$C_{18}H_{30}O_3$	18.594	294.22
9-Oxo-10(E),12(E)-octadecadienoic acid	$C_{18}H_{30}O_3$	12.847	294.22
9(Z),11(E),13(E)-octadecatrienoic acid methyl ester	$C_{19}H_{32}O_2$	16.062	292.24
9S,13R-12-oxophytodienoic acid	$C_{18}H_{28}O_3$	11.656	292.20
Monoolein	$C_{21}H_{40}O_4$	11.869	356.29
Oleamide	$C_{18}H_{35}NO$	15.422	281.27
Stearamide	$C_{18}H_{37}NO$	15.320	283.29
α-Eleostearic acid	$C_{18}H_{30}O_2$	12.448	278.22
α-Linolenic acid	$C_{18}H_{30}O_2$	14.309	278.22
Alkaloid			
4-Indolecarbaldehyde	C_9H_7NO	6.116	145.05
Amino acids			
D-Carnitine	$C_7H_{15}NO_3$	0.762	161.10
L-(+)-Arginine	$C_6H_{14}N_4O_2$	0.727	174.11
L-Glutamic acid	$C_5H_9NO_4$	0.761	147.05
L-Tyrosine	$C_9H_{11}NO_3$	0.997	181.07
L(-)-Carnitine	$C_7H_{15}NO_3$	0.760	161.10

Note: *Principal compounds

Integration of phenolic metabolite profiles with antioxidant and antibacterial activities

The biological activities of *M. malabathricum* extracts showed numerical relationships among Total Phenolic Content (TPC), antioxidant capacity, and antibacterial effectiveness. Fruit and leaf extracts had the highest TPC (140.84 and 137.20 mg GAE/g) and the lowest IC_{50} values (42.92 and 44.36 mg/L). LC-HRMS profiling identified primary phenolic metabolites, including quercetin, afzelin, kaempferol, and ellagic acid, which were more abundant in these high-TPC extracts.

Quercetin and kaempferol, which possess strong radical-scavenging activity due to their hydroxyl groups and conjugated ring structures, may have contributed to the observed low IC_{50} values. Similarly, afzelin and ellagic acid, reported to exhibit antibacterial properties by disrupting bacterial cell walls and inhibiting enzymatic activity, were present in extracts producing larger inhibition zones against *S. aureus* (up to 14.17 mm) and *E. coli* (up to 10.57 mm). In contrast, root extracts, with the lowest TPC (70.15 mg GAE/g) and minimal amounts of these metabolites, showed weaker antioxidant (IC_{50} = 89.22 mg/L) and antibacterial activities (zones 5.37-7.23 mm), supporting an association between specific phenolic metabolites and the observed biological activities.

Molecular docking study

Molecular docking was conducted to predict potential interactions between afzelin, quercetin, and trifolin with MRSA-related resistance proteins PBP2a, DdlB, and FabH. The predicted binding energies and key residues involved in these interactions are summarized in Table 7. Among the tested metabolites, quercetin showed the highest predicted binding affinity with PBP2a (-8.8 kcal/mol), while trifolin was predicted to have higher affinity for FabH (-8.6 kcal/mol) and DdlB (-6.7 kcal/mol). Additional details on residue-level interactions are provided in Table 2. The receptor-ligand interactions are further illustrated in the 2D and 3D visualizations shown in Figure 1. It should be noted that these results are computational predictions and require experimental validation to confirm biological activity against MRSA.

Discussion

Phytochemical richness and metabolite diversity

Similar to previous work by Alwash et al. (2013), *M. malabathricum* exhibited antibacterial and antioxidant activities. In this study, LC-HRMS-based metabolite profiling, correlation analysis, and in silico molecular docking were employed to provide additional information on its bioactive components and predicted molecular targets.

This study examined the antioxidant and antibacterial properties of *M. malabathricum*, with a particular focus on its phenolic compounds and their potential interactions with Methicillin-Resistant *S. aureus* (MRSA)-related proteins. These findings suggest that the plant's phenolic profile may be associated with its observed biological effects. By combining in vitro assays, molecular docking simulations, and metabolite profiling, the study provides an integrated assessment of the plant's bioactive composition. It suggests its potential as a natural antibacterial source (Hossen et al. 2024).

Phytochemical screening revealed that *M. malabathricum* contains multiple classes of metabolites, including flavonoids, phenolics, saponins, steroids, triterpenoids, alkaloids, and coumarins. These compounds are well known for their diverse pharmacological properties, including antioxidant, antibacterial, and anti-inflammatory activities (Isnaini et al. 2023; Tan et al. 2024). As shown in Table 2, all plant parts contained flavonoids and phenolics, the main metabolites associated with antioxidant and antibacterial functions. In particular, alkaloids and saponins were more abundant in flowers, roots, and fruits, which supports their possible contribution to the plant's biological activities (Zakaria et al. 2022; Hipol et al. 2023).

LC-HRMS profiling (Table 3) further confirms the plant's chemical diversity, identifying major metabolites such as quercetin, afzelin, trifolin, and ursolic acid, all of which have previously been linked to antioxidant and antibacterial activity (El-Ghorab et al. 2022; Lee et al. 2024). The higher concentrations of alkaloids and saponins in flowers could partly explain their stronger antimicrobial behavior despite moderate phenolic levels (Hamilton-Amachree and Odokwo 2023). Therefore, the biological activity of *M. malabathricum* likely results from synergistic effects among several metabolite classes rather than phenolics alone (Rusli et al. 2022). While the LC-HRMS results provided a valuable overview of the chemical profile, the metabolite assignments remain tentative due to the absence of reference standards. Future analyses incorporating MS/MS confirmation and authentic compound comparisons are recommended to improve the reliability of compound identification.

Table 4. Total phenolic content of *Melastoma malabathricum* extracts

Sample	TPC (mg GAE/g)
Leaf	137.20 ± 0.22^{c}
Root	70.15 ± 1.36^{a}
Flower	93.30 ± 0.22^{b}
Fruit	$140.84\pm0,22^{d}$

Note: Error bars represent SD (n = 3). Different letters denote significant differences ($p<0.05$; ANOVA with Duncan's post-hoc test)

Table 5. Antioxidant activity of *Melastoma malabathricum* extracts measured using the DPPH assay

Sample	IC_{50} value (mg/L)
Leaf	44.36 ± 0.17^{f}
Root	89.22 ± 0.47^{h}
Flower	62.13 ± 0.88^{h}
Fruit	42.92 ± 0.07^{f}
Ascorbic acid	36.04 ± 0.11^{e}

Note: Values represent mean±SD (n = 3). Different superscript letters denote statistically significant differences among samples ($p<0.05$; one-way ANOVA followed by Duncan's post-hoc test)

Table 6. Inhibition zones of *Melastoma malabathricum* extracts (mm)

Microorganisms	Leaf	Stem	Root	Flower	DMSO	Ampicillin
Gram-positive bacteria						
Staphylococcus aureus (MSSA)	7.87 ± 0.25^{q}	12.23 ± 0.47^{r}	5.37 ± 1.10^{p}	14.17 ± 0.06^{s}	0.00 ± 0.00	21.65 ± 0.64
Gram-negative bacteria						
Escherichia coli	10.57 ± 1.06^{q}	9.80 ± 1.21^{q}	7.23 ± 0.45^{p}	9.67 ± 0.31^{q}	0.00 ± 0.00	21.03 ± 1.46

Note: Data are expressed as mean±SD (n = 3). Different superscript letters within the same row indicate statistically significant differences ($p<0.05$, one-way ANOVA followed by Duncan's multiple range test). The negative control (0.1% DMSO) showed no inhibitory activity

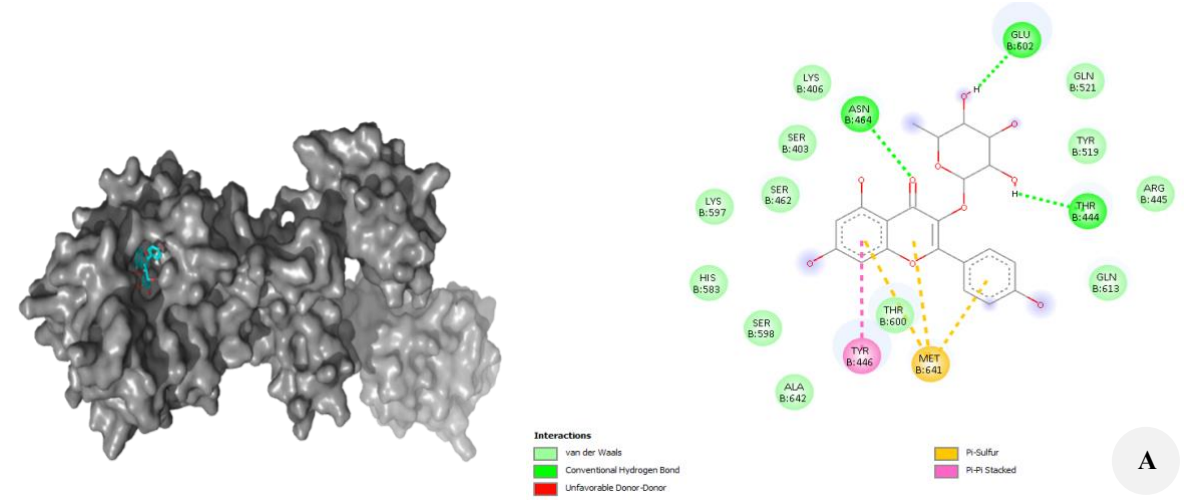
GLU B:602
LYS B:406
GLN B:521
ASN B:464
SER B:403
TYR B:519
SER B:462
ARG B:445
LYS B:597
THR B:444
HIS B:583
GLN B:613
THR B:600
SER B:598
TYR B:446
MET B:641
ALA B:642
Interactions
van der Waals
Conventional Hydrogen Bond
Unfavorable Donor-Donor
Pi-Sulfur
Pi-Pi Stacked
A

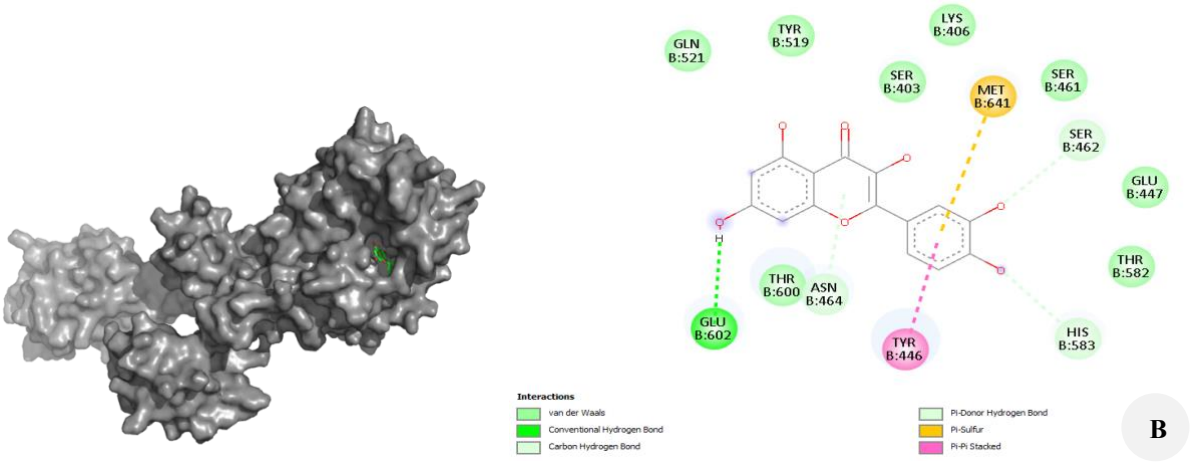
LYS B:406
GLN B:521
TYR B:519
SER B:403
MET B:641
SER B:461
SER B:462
GLU B:447
THR B:582
THR B:600
ASN B:464
GLU B:602
TYR B:446
HIS B:583
Interactions
van der Waals
Conventional Hydrogen Bond
Carbon Hydrogen Bond
Pi-Donor Hydrogen Bond
Pi-Sulfur
Pi-Pi Stacked
B

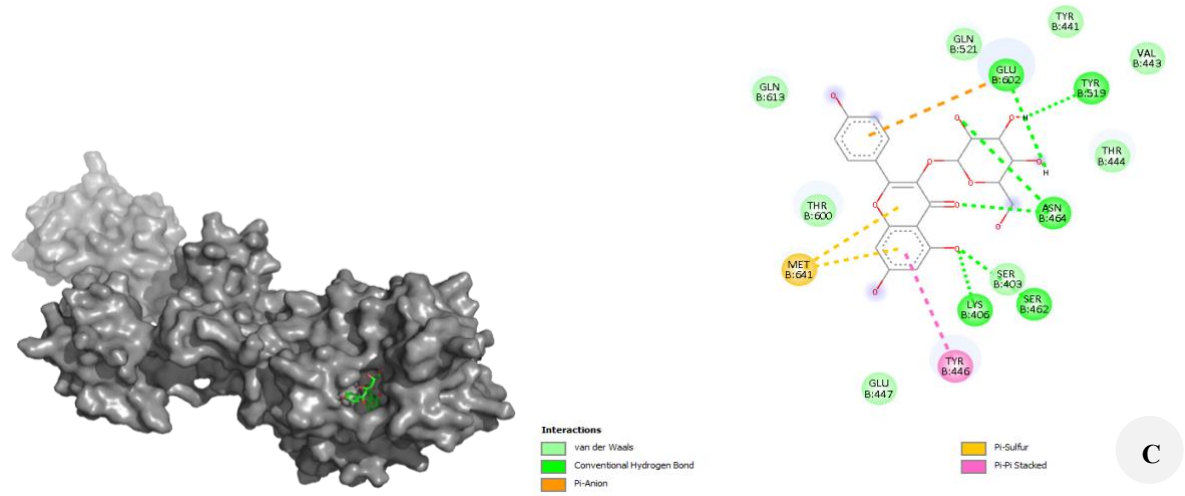
TYR B:441
GLN B:521
VAL B:443
GLU B:602
GLN B:613
TYR B:519
THR B:444
THR B:600
ASN B:464
MET B:641
SER B:403
LYS B:406
SER B:462
TYR B:446
GLU B:447
Interactions
van der Waals
Conventional Hydrogen Bond
Pi-Anion
Pi-Sulfur
Pi-Pi Stacked
C

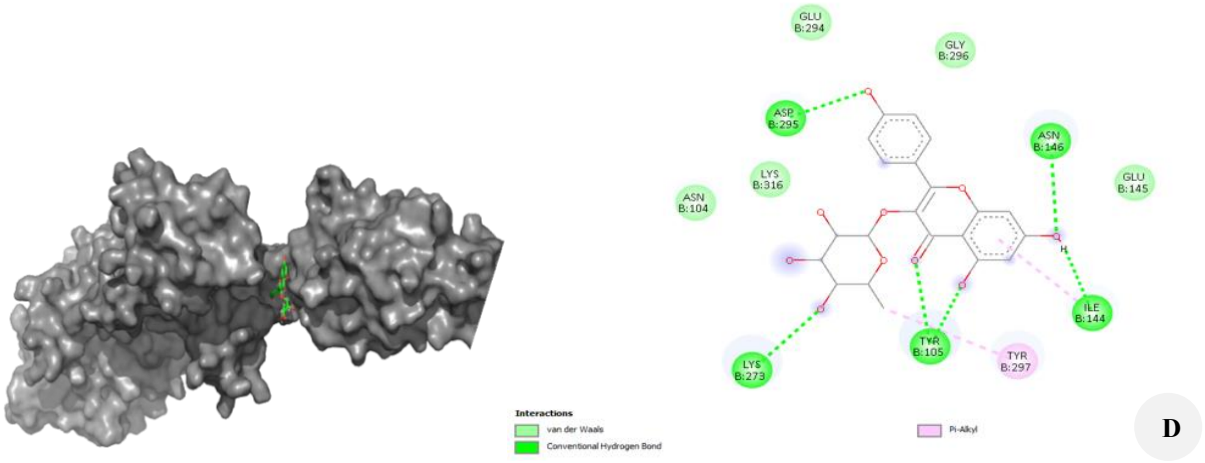
GLU B:294
GLY B:296
ASP B:295
ASN B:146
LYS B:316
GLU B:145
ASN B:104
ILE B:144
TYR B:105
TYR B:297
LYS B:273
Interactions
van der Waals
Conventional Hydrogen Bond
Pi-Alkyl

D

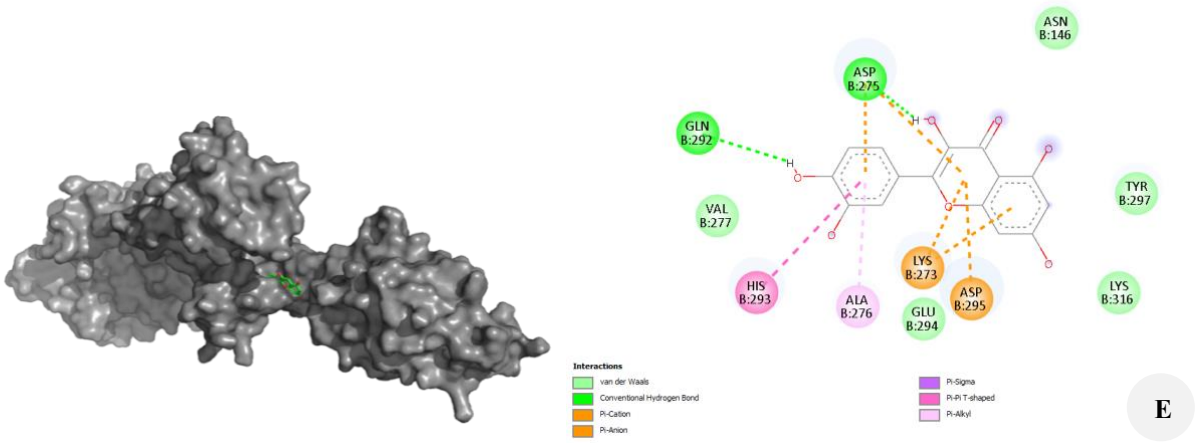
ASN B:146
ASP B:275
GLN B:292
TYR B:297
VAL B:277
LYS B:273
HIS B:293
ALA B:276
ASP B:295
GLU B:294
LYS B:316
Interactions
van der Waals
Conventional Hydrogen Bond
Pi-Cation
Pi-Anion
Pi-Sigma
Pi-Pi T-shaped
Pi-Alkyl

E

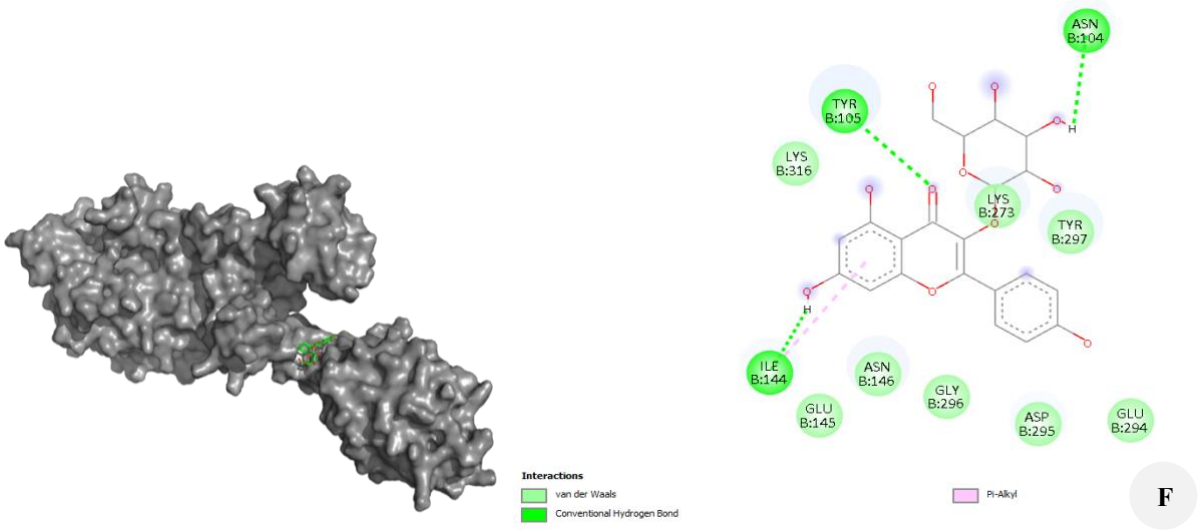
ASN B:104
TYR B:105
LYS B:316
LYS B:273
TYR B:297
ILE B:144
ASN B:146
GLY B:296
GLU B:145
ASP B:295
GLU B:294
Interactions
van der Waals
Conventional Hydrogen Bond
Pi-Alkyl

F

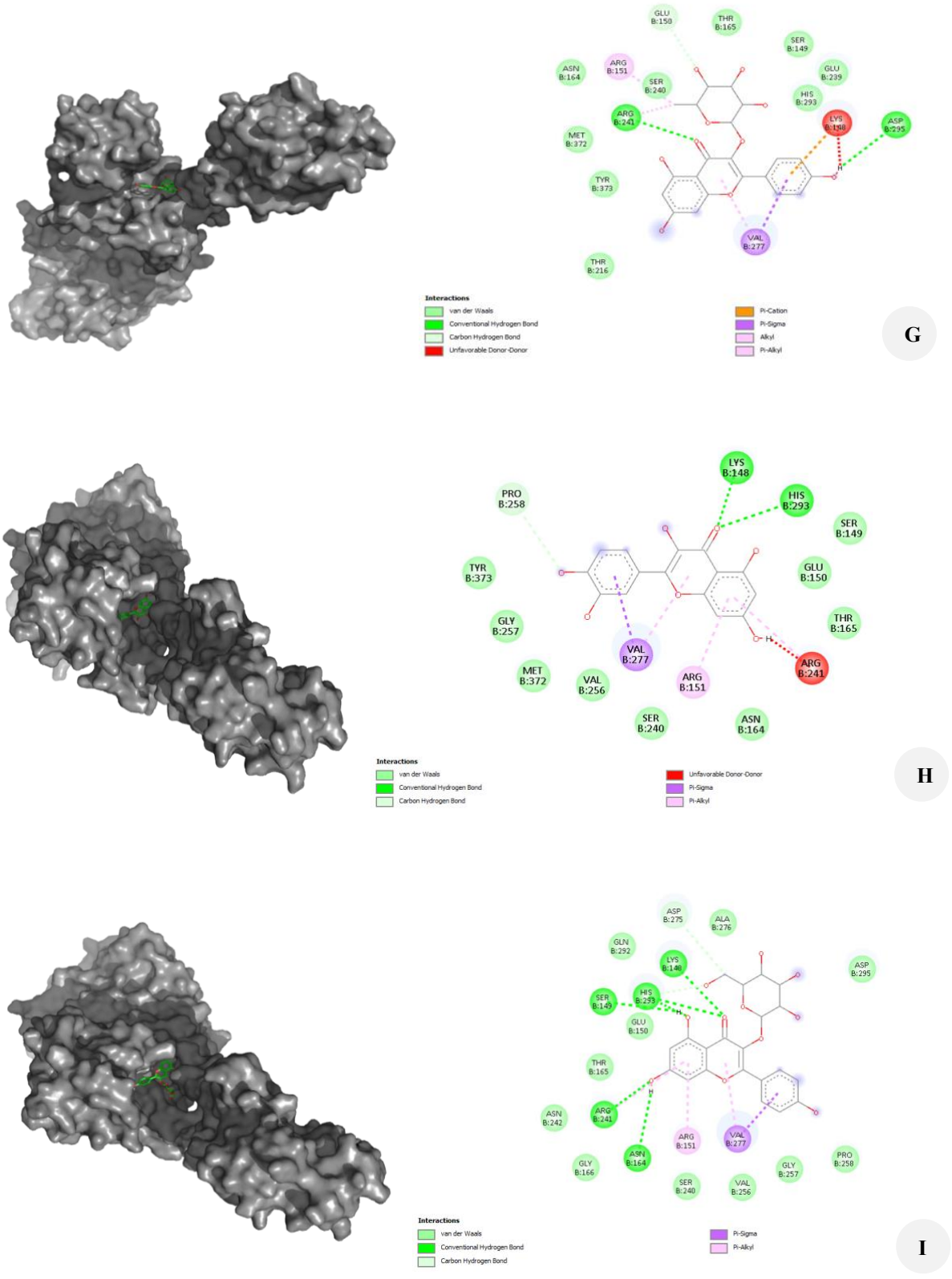

Figure 1. 2D and 3D visualization of receptor-ligand interactions for MRSA proteins (afzelin, quercetin, and trifolin). These figures show the binding interfaces between the metabolites and target proteins PBP2a, DdlB, and FabH, highlighting the key residues involved in the interactions. A. 4JCN - Afzelin, B. 1MWT - Quercetin, C. 1MWT - Trifolin, D. 4JCN - Afzelin, E. 4JCN - Quercetin, F. 4JCN - Trifolin, G. 5M18 - Afzelin, H. 5M18 - Quercetin, I. 5M18 - Trifolin

Table 7. Residue-level binding interactions of trifolin, quercetin, and afzelin with MRSA resistance proteins

Protein	Compound	Binding affinity (Kcal/mol)	RMSD	H bond	Hydrophobic	Other interactions
1MWT	Afzelin	-8,1	1.201	**Glu602, Asn464, Thr444**, Gln521	Lys406, Ser403, Ser462, Lys597, His583, Ser598, Ala642, Tyr519, Arg445, Gln613	Met641, Tyr446
	Quercetin	-8.8	0.574	**Glu602, Asn464, Ser462**, Glu447, Thr582, His583	Lys406, Ser403, Ser461, Tyr519, Gln521	Met641, Tyr446
	Trifolin	-8.0	1.256	**Glu602, Asn464, Thr444**	Lys406, Ser403, Ser462, Tyr519, Lys597, His583, Ser598, Thr600, Ala642, Arg445, Gln613	Met641, Tyr446
4JCN	Afzelin	-6.3	1.948	**Asp295, Asn146, Lys273**, Tyr105, Ile144	Asn104, Lys316, Glu294, Gly296, Glu145	Tyr297
	Quercetin	-6.7	1.436	**Gln292, Asp275**	Val277, Asn146, Tyr297, Lys316	Lys273, Asp295, Glu294, His293, Ala276
	Trifolin	-6.1	1.743	**Tyr105, Asn104, Ile144**, Lys273	Asn146, Glu145, Glu294, Asp295, Gly296, Tyr297, Lys316	
5M18	Afzelin	-7.6	1.346	**Arg241, Asp295**	Asn164, Met372, Tyr373, Thr216, Glu150, Thr165, Ser149, Glu239, His293	Lys148, Val277, Arg151, Ser240), Lys148
	Quercetin	-7.8	1.360	**Lys148, His293**	Pro258, Tyr373, Met372, Val256, Gly257, Ser240, Asn164, Glu150, Thr165, Ser149	Val277, Arg151, Arg241
	Trifolin	-8.6	1.969	**Lys148, His293, Glu150**, Arg241, Asn164, Ser149	Asp275, Ala276, Asn242, Gln292, Thr165, Gly166, Gly257, Val256, Ser240, Pro258	Val277, Arg151

Note: More negative values indicate stronger binding affinity. RMSD: Root mean square deviation

Extraction yields (Table 1) also support this chemical richness. Flowers and leaves exhibited the highest yields (6.08% and 5.15%), consistent with previous reports indicating that aerial plant parts tend to accumulate higher levels of secondary metabolites, possibly due to greater exposure to environmental stressors such as ultraviolet radiation and herbivore activity (Boutaoui et al. 2018; García-Pérez et al. 2020; Alcalde et al. 2022). Methanol extraction proved particularly efficient, as the solvent can extract both polar and moderately non-polar compounds (Truong et al. 2019; Baeshen et al. 2023; Riyadi et al. 2023; Ghaffar and Perveen 2024). Collectively, these results suggest that metabolite diversity may contribute to the plant's antioxidant and antibacterial activities, supporting its potential pharmacological relevance.

Antioxidant-antibacterial correlation

The relationships among phenolic composition, antioxidant capacity, and antibacterial activity were further evaluated. The Total Phenolic Content (TPC) and antioxidant results (Tables 4-5) revealed that fruits and leaves with higher TPC values exhibited stronger radical-scavenging capacity, whereas roots showed weaker activity. These results align with the established mechanism, in which phenolic hydroxyl groups and conjugated aromatic structures contribute to electron donation and radical stabilization (El-Ghorab et al. 2022).

Interestingly, flower extracts showed strong antioxidant potential despite moderate TPC, suggesting that non-phenolic constituents such as alkaloids and flavonoids also contribute significantly to antioxidant effects (Ismail et al. 2021; Apridamayanti et al. 2022; Lestari et al. 2022; Hosni et al. 2023). This observation supports a synergistic mechanism involving multiple compound classes.

Furthermore, antibacterial assays (Table 6) demonstrated that flower extracts produced the largest inhibition zones against *S. aureus* (MSSA) (14.17 mm) and *E. coli* (9.67 mm), whereas root extracts were least effective. The flower extract showed apparent antimicrobial activity despite its comparatively lower TPC, suggesting that phenolics are unlikely to be the sole contributors to this activity. This pattern indicates that antibacterial performance depends not only on phenolics but also on alkaloids and saponins, which are abundant in floral tissues (Dwivedi et al. 2020; Vittaya et al. 2023). Such metabolites may enhance membrane permeability or inhibit bacterial enzymes, complementing phenolic-based mechanisms (Okmen et al. 2023).

Although the Total Phenolic Content (TPC) was highest in the fruit extract, followed by the leaf, flower, and root extracts, the most potent antibacterial activity was observed in the flower extract. It suggests that non-phenolic metabolites also contribute to antibacterial efficacy, indicating that phenolic content alone does not fully explain the observed activity.

A strong negative correlation between TPC and antioxidant IC_{50} values ($r = -0.97$, $p = 0.03$) confirms that higher phenolic levels are associated with stronger antioxidant capacity (Osman et al. 2020; Lyu et al. 2022; Kalpoutzakis et al. 2023). Regression analysis yielded the model $IC_{50} = 126.42 - 0.61 \times TPC$ ($R^2 = 0.93$, $F = 28.05$, $p = 0.03$), indicating that variations in TPC explain 93% of the observed antioxidant differences. Positive but non-significant correlations between TPC and antibacterial activities ($r = 0.30$, $p = 0.70$ for *S. aureus*; $r = 0.84$, $p = 0.16$ for *E. coli*) suggest that phenolic compounds may contribute to antibacterial effects, yet their influence alone is unclear. Thus, other metabolites likely modulate the overall bioactivity.

The LC-HRMS data further confirm the link between phenolic composition and bioactivity. Extracts richer in phenolics showed more potent antioxidant and antibacterial effects and contained well-known bioactive molecules such as quercetin and kaempferol. These flavonols can donate electrons to neutralize free radicals and interact with bacterial components through π-π stacking and hydrophobic bonding (Liu et al. 2022; Yang et al. 2024). Afzelin and ellagic acid, also identified, may enhance activity through improved solubility and complementary inhibition (Kciuk et al. 2024). Collectively, the dual antioxidant-antibacterial effects of *M. malabathricum* appear to arise from synergistic interactions among phenolic derivatives, particularly quercetin-type compounds (Pratiwi et al. 2021). Further quantitative analyses and correlations with docking results could deepen understanding of these mechanisms.

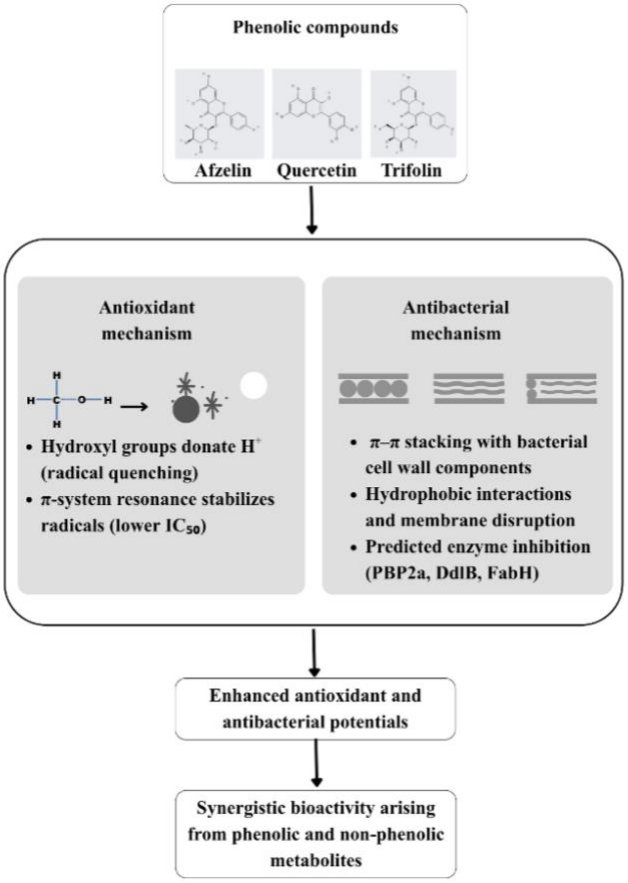

Figure 2. Proposed mechanistic framework illustrating how phenolic compounds (e.g., quercetin, afzelin, and trifolin) contribute to antioxidant activity and predicted antibacterial effects through radical scavenging and potential interactions with MRSA-related resistance proteins

Docking and molecular implications

Molecular docking complemented the experimental results by predicting how selected metabolites might interact with MRSA resistance-related proteins (PBP2a, DdlB, and FabH). Among the docked compounds, quercetin showed the strongest predicted affinity toward PBP2a (-8.8 kcal/mol), while trifolin bound firmly to FabH (-8.6 kcal/mol) and DdlB (-6.7 kcal/mol). These predicted interactions suggest potential inhibition of bacterial cell wall and fatty acid synthesis (Aribisala and Sabiu 2022; Li et al. 2023).

Furthermore, quercetin's predicted binding to PBP2a may interfere with the enzyme's β-lactam resistance mechanism (Islam et al. 2024). Trifolin's interaction with FabH suggests possible disruption of lipid biosynthesis (Sanyal et al. 2019), while afzelin's docking with DdlB points to potential inhibition of peptidoglycan synthesis (Lotha et al. 2018). Although the docking simulations provide plausible molecular insights, the results remain computational and require experimental validation. The docking analysis did not include standard reference antibiotics (e.g., vancomycin) as positive controls for benchmarking binding affinities, which limits the comparative interpretation of the predicted binding energy values. This study did not experimentally test the inhibitory effects of these compounds against MRSA strains; therefore, additional biochemical and microbiological validation is necessary to confirm their biological relevance.

The low binding energy for trifolin's interaction with DdlB suggests a stable binding conformation, supporting the predicted docking model (Jiang et al. 2024). Hence, further molecular dynamics simulations and biochemical validation are needed to confirm the relevance of these interactions (Vidal-Limon et al. 2022). Overall, the in silico findings complement the experimental results and provide a preliminary mechanistic perspective on the antibacterial potential of *M. malabathricum*.

A mechanistic model summarizing the proposed relationships between phenolic composition, antioxidant capacity, and antibacterial potential is illustrated in Figure 2. Phenolics such as quercetin and afzelin stabilize radical intermediates and may disrupt bacterial structures via π-π interactions and hydrophobic binding, as well as engage MRSA-related resistance proteins (Yang et al. 2022; Calinsky and Levy 2024). These proposed mechanisms are predictive and should be validated in future molecular and microbiological experiments.

In conclusion, the integrated results indicate that phenolic compounds, particularly quercetin derivatives, may contribute to the antioxidant and antibacterial activities observed in *M. malabathricum*. The docking analyses suggest possible interactions between these metabolites and MRSA resistance-related proteins (PBP2a, DdlB, and FabH), providing an initial mechanistic hypothesis that requires further experimental confirmation. These interpretations should be viewed cautiously due to the limited number of replicates and small sample size, which may affect the statistical robustness of the findings. Nonetheless, this study offers a preliminary foundation for future investigations involving MRSA clinical isolates, molecular dynamics simulations, and targeted enzymatic assays to validate the predicted interactions and further elucidate the antibacterial potential of *M. malabathricum*.

ACKNOWLEDGEMENTS

The authors are grateful to the Directorate of Research and Community Service, Directorate General of Research and Development, Ministry of Higher Education, Science, and Technology for supporting this research through the 2025 Doctoral Dissertation Research Scheme (PDD), with research contract number: 060/C3/DT.05.00/PL/2025. The authors also acknowledge the facilities and scientific and technical support from Advanced Characterization Laboratories, Yogyakarta, Indonesia, National Research and Innovation Agency, through E-Layanan Sains BRIN.

REFERENCES

Alcalde MA, Perez-Matas E, Escrich A, Cusido RM, Palazon J, Bonfill M. 2022. Biotic eliciters in adventitious and hairy root cultures: A review from 2010 to 2022. Molecules 27 (16): 5253. DOI: 10.3390/molecules27165253.

Alwash MS, Ibrahim N, Ahmad WY. 2013. Bio-guided study on *Melastoma malabathricum* Linn leaves and elucidation of its biological activities. Am J Appl Sci 10 (8): 767-778. DOI: 10.3844/ajassp.2013.767.778.

Apridamayanti P, Pratiwi L, Sari R. 2022. Gas chromatography study of n-hexane and chloroform fractions of ethanol extract of *Melastoma malabathricum* L. leaves: An in vitro study of antioxidant and SPF values. Intl J Pharm Pharm Sci 14 (3): 40-46. DOI: 10.22159/ijpps.2022v14i3.43801.

Aribisala JO, Sabiu S. 2022. Cheminformatics identification of phenolics as modulators of penicillin-binding protein 2a of *Staphylococcus aureus*: A structure-activity-relationship-based study. Pharmaceutics 14 (9): 1818. DOI: 10.3390/pharmaceutics14091818.

Azizan FF, Hanafiah RM, Msarah MJ, Md. Nor NS, Ibrahim N, Aqma WS. 2020. Antibacterial and antibiofilm analyses of *Melastoma malabathricum* leaves extract against *Streptococcus mutans* on tooth surfaces. Malays J Microbiol 16: 454-460. DOI: 10.21161/mjm.190678.

Baeshen NA, Almulaiky YQ, Afifi M, Al-Farga A, Ali HA, Baeshen NN, Abomughaid MM, Abdelazim AM, Baeshen MN. 2023. GC-MS analysis of bioactive compounds extracted from plant *Rhazya stricta* using various solvents. Plants 12: 960. DOI: 10.3390/plants12040960.

Bouarab-Chibane L, Forquet V, Lantéri P, Clément Y, Léonard-Akkari L, Oulahal N, Degraeve P, Bordes C. 2019. Antibacterial properties of polyphenols: Characterization and QSAR (quantitative structure-activity relationship) models. Front Microbiol 10: 829. DOI: 10.3389/fmicb.2019.00829.

Boutaoui N, Zaiter L, Benayache F, Benayache S, Cacciagrano F, Cesa S, Secci D, Carradori S, Giusti AM, Campestre C, Menghini L, Locatelli M. 2018. *Atriplex mollis* Desf. aerial parts: Extraction procedures, secondary metabolites, and color analysis. Molecules 23 (8): 1962. DOI: 10.3390/molecules23081962.

Calinsky R, Levy Y. 2024. Aromatic residues in proteins: Re-evaluating the geometry and energetics of π-π, cation-π, and CH-π interactions. J Phys Chem B 128 (36): 8687-8700. DOI: 10.1021/acs.jpcb.4c04774.

Chaachouay N, Zidane L. 2024. Plant-derived natural products: A source for drug discovery and development. Drugs Drug Candidates 3 (1): 184-207. DOI: 10.3390/ddc3010011.

CLSI [Clinical and Laboratory Standards Institute]. 2023. Performance standards for antimicrobial susceptibility testing. Clinical and Laboratory Standards Institute. www.nih.org.pk.

da Cruz Nizer WS, Adams ME, Allison KN, Montgomery MC, Mosher H, Cassol E, Overhage J. 2024. Oxidative stress responses in biofilms. Biofilm 7: 100203. DOI: 10.1016/j.bioflm.2024.100203.

Dwivedi MK, Sonter S, Mishra S, Patel DK, Singh PK. 2020. Antioxidant, antibacterial activity, and phytochemical characterization of *Carica papaya* flowers. Beni-Suef Univ J Basic Appl Sci 9: 23. DOI: 10.1186/s43088-020-00048-w.

El-Ghorab AH, Behery FA, Abdelgawad MA, Alsohaimi IH, Musa A, Mostafa EM, Altaleb HA, Althobaiti IO, Hamza M, Elkomy MH, Hamed AA, Sayed AM, Hassan HM, Aboseada MA. 2022. LC/MS profiling and gold nanoparticle formulation of major metabolites from *Origanum majorana* as antibacterial and antioxidant potentialities. Plants 11 (14): 1871. DOI: 10.3390/plants11141871.

García-Pérez P, Lozano-Milo E, Landín M, Gallego PP. 2020. Combining medicinal plant in vitro culture with machine learning technologies for maximizing the production of phenolic compounds. Antioxidants 9 (3): 210. DOI: 10.3390/antiox9030210.

Ghaffar N, Perveen A. 2024. Solvent polarity effects on extraction yield, phenolic content, and antioxidant properties of Malvaceae family seeds: A comparative study. N Z J Bot 63 (4): 627-637. DOI: 10.1080/0028825x.2024.2392705.

Hamilton-Amachree A, Odokwo EO. 2023. Antioxidant and antimicrobial activities of floral methanolic extract of *Costus lucanusianus*. Asian J Appl Chem Res 14 (1): 1-7. DOI: 10.9734/ajacr/2023/v14i1254.

Hipol RL, Wayas H, Hipol R, Bacuyag FM, Cabanlong J, Daquigan M, Pladio L. 2023. Phytochemical content, thin layer chromatographic profile, and pharmacologic activities of the Philippine native *Melastoma malabathricum* Linn. from Benguet. Sci Eng Health Stud 17: 23050012. DOI: 10.69598/sehs.17.23050012.

Hosni S, Abd Gani SS, Orsat V, Hassan M, Abdullah S. 2023. Ultrasound-assisted extraction of antioxidants from *Melastoma malabathricum* Linn.: Modeling and optimization using Box-Behnken design. Molecules 28 (2): 487. DOI: 10.3390/molecules28020487.

Hossen SMM, Eva TA, Karim MS, Mamurat H, Rahat MHH, Nipun TS. 2024. Antimicrobial potential, GC-MS analysis and molecular docking studies of *Coelogyne suaveolens* extracts: Identification of bioactive compounds with mechanism of action. Biochem Biophys Rep 37: 101648. DOI: 10.1016/j.bbrep.2024.101648.

Islam MR, Azmal M, Prima FS, Zaman B, Hossain MM, Mishu MA, Ghosh A. 2024. Retention of methicillin susceptibility in *Staphylococcus aureus* using natural adjuvant as an allosteric modifier of penicillin-binding protein 2a. Comput Biol Med 181: 109070. DOI: 10.1016/j.compbiomed.2024.109070.

Ismail NH, Amira NH, Latip SNHM, Zain WZWM, Aani SNA, Aziman NA. 2021. Phytochemical screening and antioxidant activity of *Melastoma malabathricum* and *Chromolaena odorata* by DPPH radical scavenging method. Food Res 5 (S4): 30-37. DOI: 10.26656/fr.2017.5(S4).006.

Isnaini, Oktaviyanti IK, Budiarti LY. 2023. Antibacterial and wound healing activity of ethanolic extract *Melastoma malabathricum* L. Res J Pharm Technol 16 (5): 2210-2214. DOI: 10.52711/0974-360X.2023.00363.

Itam A, Wati MS, Agustin V, Sabri N, Jumanah RA, Efdi M. 2021. Comparative study of phytochemical, antioxidant, and cytotoxic activities and phenolic content of *Syzygium aqueum* (Burm. f. Alston f.) extracts growing in West Sumatera, Indonesia. Sci World J 2021: 5537597. DOI: 10.1155/2021/5537597.

Jiang Y, Deane CM, Morris GM, O'Brien EP. 2024. It is theoretically possible to avoid misfolding into non-covalent lasso entanglements using small molecule drugs. PLoS Comput Biol 20 (3): e1011901. DOI: 10.1371/journal.pcbi.1011901.

Kalpoutzakis E, Chatzimitakos T, Athanasiadis V, Mitakou S, Aligiannis N, Bozinou E, Gortzi O, Skaltsounis LA, Lalas SI. 2023. Determination of the total phenolics content and antioxidant activity of extracts from parts of plants from the Greek island of Crete. Plants 12 (5): 1092. DOI: 10.3390/plants12051092.

Kciuk M, Garg N, Dhankhar S, Saini M, Mujwar S, Devi S, Chauhan S, Singh TG, Singh R, Marciniak B, Gielecińska A, Kontek R. 2024. Exploring the comprehensive neuroprotective and anticancer potential of afezlin. Pharmaceuticals 17 (6): 701. DOI: 10.3390/ph17060701.

Kumar AP, Murali V, Nagaraju K, Srinivas M. 2023. Fungal endophytes: A potential application in integrated plant health management. Intl J Plant Soil Sci 35: 1570-1578. DOI: 10.9734/ijpss/2023/v35i183427.

Kumar V, Sachan R, Rahman M, Rub RA, Patel DK, Sharma K, Gahtori P, Al-Abbasi FA, Alhayyani S, Anwar F, Kim HS. 2021. Chemopreventive effects of *Melastoma malabathricum* L. extract in mammary tumor model via inhibition of oxidative stress and inflammatory cytokines. Biomed Pharmacother 137: 111298. DOI: 10.1016/j.biopha.2021.111298.

Lade H, Kim J-S. 2023. Molecular determinants of β-lactam resistance in Methicillin-Resistant *Staphylococcus aureus* (MRSA): An updated review. Antibiotics 12 (9): 1362. DOI: 10.3390/antibiotics12091362.

Lafraxo S, El Barnossi A, El Moussaoui A, Bourhia M, Salamatullah AM, Alzahrani A, Akka AA, Choubbane A, Akhazzane M, Aboul-Soud MAM, Giesy JP, Bari A. 2022. Essential oils from leaves of *Juniperus thurifera* L., exhibiting antioxidant, antifungal and antibacterial activities against antibiotic-resistant microbes. Horticulturae 8 (4): 321. DOI: 10.3390/horticulturae8040321.

Lawag IL, Nolden ES, Schaper AAM, Lim LY, Locher C. 2023. A modified Folin-Ciocalteu assay for the determination of total phenolics content in honey. Appl Sci 13 (4): 2135. DOI: 10.3390/app13042135.

Lee AS, de Lencastre H, Garau J, Kluytmans J, Malhotra-Kumar S, Peschel A, Harbarth S. 2018. Methicillin-resistant *Staphylococcus aureus*. Nat Rev Dis Primers 4: 18033. DOI: 10.1038/nrdp.2018.33.

Lee J, Kim HS, Park JW, Yun B, Bang WY, Moon KH, Seo Y. 2024. Exploration of new drug candidate derived from antioxidants of Korean native halophytes: Control of *Acinetobacter baumannii* with antipathogenic activity. Antioxidants 13 (11): 1134. DOI: 10.3390/antiox13111334.

Lestari OA, Palupi NS, Setiyono A, Kusnandar F, Yuliana ND. 2022. In vitro antioxidant potential and phytochemical profiling of *Melastoma malabathricum* leaf water extract. Food Sci Technol 42: e92021. DOI: 10.1590/fst.92021.

Li X, Cai Y, Xia Q, Liao Y, Qin R. 2023. Antibacterial sensitizers from natural plants: A powerful weapon against methicillin-resistant *Staphylococcus aureus*. Front Pharmacol 14: 1118793. DOI: 10.3389/fphar.2023.1118793.

Liu D-L, Liu S-J, Hu S-Q, Chen Y-C, Guo J. 2022. Probing the potential mechanism of quercetin and kaempferol against heat stress-induced Sertoli cell injury: Integrating network pharmacology and experimental validation. Intl J Mol Sci 23: 11163. DOI: 10.3390/ijms231911163.

Lotha R, Sundaramoorthy NS, Shamprasad BR, Nagarajan S, Sivasubramanian A. 2018. Plant nutraceuticals (quercetrin and afzelin) capped silver nanoparticles exert potent antibiofilm effect against food borne pathogen *Salmonella enterica* serovar Typhimurium and curtail planktonic growth in zebrafish infection model. Microb Pathog 120: 109-118. DOI: 10.1016/j.micpath.2018.04.044.

Lyu JI, Ryu J, Seo K-S, Kang K-Y, Park SH, Ha TH, Ahn J-W, Kang S-Y. 2022. Comparative study on phenolic compounds and antioxidant activities of hop (*Humulus lupulus* L.) strobile extracts. Plants 11 (1): 135. DOI: 10.3390/plants11010135.

Okmen G, Giannetto D, Fazio F, Arslan K. 2023. Investigation of Pomegranate (*Punica granatum* L.) flowers' antioxidant properties and antibacterial activities against different *Staphylococcus* species associated with bovine mastitis. Vet Sci 10 (6): 394. DOI: 10.3390/vetsci10060394.

Osman MA, Mahmoud GI, Shoman SS. 2020. Correlation between total phenols content, antioxidant power and cytotoxicity. Biointerface Res Appl Chem 11: 10640-10653. DOI: 10.33263/briac113.1064010653.

Pisano MB, Kumar A, Medda R, Gatto G, Pal R, Fais A, Era B, Cosentino S, Uriarte E, Santana L, Pintus F, Matos MJ. 2019. Antibacterial activity and molecular docking studies of a selected series of hydroxy-3-arylcoumarins. Molecules 24: 2815. DOI: 10.3390/molecules24152815.

Pratiwi L, Sari R, Apridamayanti P. 2021. Synergistic interaction of ethyl acetate fraction from *Melastoma malabathricum* L. leaves in combination with ciprofloxacin and gentamicin against *Escherichia coli* isolated from diabetic foot ulcer patients. Trad Med J 26 (1): 63-70. DOI: 10.22146/mot.57399.

Ramli NW, Zain WZWM, Ab Wahab MZ, Hamid N, Abdullah NA, Zamanhuri N. 2022. Phytochemical screening, antioxidant and antifungal activity of methanolic extract of *Fimbristylis dichotoma* and *Fimbristylis miliacea*. IOP Conf Ser: Earth Environ Sci 1059: 012080. DOI: 10.1088/1755-1315/1059/1/012080.

Riyadi PH, Susanto E, Anggo AD, Arifin MH, Rizki L. 2023. Effect of methanol solvent concentration on the extraction of bioactive compounds using Ultrasonic-Assisted Extraction (UAE) from *Spirulina platensis*. Food Res 7: 59-66. DOI: 10.26656/fr.2017.7(s3).9.

Rusli LS, Abdullah R, Yaacob JS, Osman N. 2022. Organic amendments effects on nutrient uptake, secondary metabolites, and antioxidant properties of *Melastoma malabathricum* L. Plants 11 (2): 153. DOI: 10.3390/plants11020153.

Sanyal R, Singh V, Harinarayanan R. 2019. A novel gene contributing to the initiation of fatty acid biosynthesis in *Escherichia coli*. J Bacteriol 201 (19): e00354-19. DOI: 10.1128/jb.00354-19.

Shah KN, Shah PN, Agobe FO, Lovato K, Gao H, Ogun O, Hoffman C, Yabe-Gill M, Chen Q, Sweatt J, Chirra B, Muñoz-Medina R, Farmer DE, Kürti L, Cannon CL. 2024. Antimicrobial activity of a natural compound and analogs against multi-drug-resistant gram-positive

pathogens. Microbiol Spectr 12 (3): e0151522. DOI: 10.1128/spectrum.01515-22.

Shoaib M, Aqib AI, Muzammil I, Majeed N, Bhutta ZA, Kulyar MF-E-A, Fatima M, Zaheer C-NF, Muneer A, Murtaza M, Kashif M, Shafqat F, Pu W. 2023. MRSA compendium of epidemiology, transmission, pathophysiology, treatment, and prevention within one health framework. Front Microbiol 13: 1067284. DOI: 10.3389/fmicb.2022.1067284.

Tan YJ, Koh SP, Khozirah S, Rozaihan M, Jacob M, Khirrol NAW, Mohd-Shaharizan MS, Tan GH. 2024. Antibacterial effect of *Melastoma malabathricum* leaves extract against locally isolated bovine mastitis pathogens. Food Res 8 (Suppl 3): 13-24. DOI: 10.26656/fr.2017.8(s3).2.

Truong D-H, Nguyen DH, Ta NTA, Bui AV, Do TH, Nguyen HC. 2019. Evaluation of the use of different solvents for phytochemical constituents, antioxidants, and in vitro anti-inflammatory activities of *Severinia buxifolia*. J Food Qual 2019 (1): 8178294. DOI: 10.1155/2019/8178294.

Vaishampayan A, Grohmann E. 2022. Antimicrobials functioning through ROS-mediated mechanisms: Current insights. Microorganisms 10 (1): 61. DOI: 10.3390/microorganisms10010061.

Verma AK, Ahmed SF, Hossain MS, Bhojiya AA, Mathur A, Upadhyay SK, Srivastava AK, Vishvakarma NK, Barik M, Rahaman MM, Bahadur NM. 2022. Molecular docking and simulation studies of flavonoid compounds against PBP-2a of methicillin-resistant *Staphylococcus aureus*. J Biomol Struct Dyn 40 (21): 10561-10577. DOI: 10.1080/07391102.2021.1944911.

Vidal-Limon A, Aguilar-Toalá JE, Liceaga AM. 2022. Integration of molecular docking analysis and molecular dynamics simulations for studying food proteins and bioactive peptides. J Agric Food Chem 70 (4): 934-943. DOI: 10.1021/acs.jafc.1c06110.

Vittaya L, Chalad C, Ratsameepakai W, Leesakul N. 2023. Phytochemical characterization of bioactive compounds extracted with different solvents from *Calophyllum inophyllum* flower and activity against pathogenic bacteria. S Afr J Bot 154: 346-355. DOI: 10.1016/j.sajb.2023.01.052.

Windarsih A, Suratno, Warmiko HD, Indrianingsih AW, Rohman A, Ulumuddin YI. 2022. Untargeted metabolomics and proteomics approach using liquid chromatography-orbitrap high resolution mass spectrometry to detect pork adulteration in *Pangasius hypopthalmus* meat. Food Chem 386: 132856. DOI: 10.1016/j.foodchem.2022.132856.

Yang J-Q, Chen H-J, Huang C-R, Chen C-S, Chen Y-F. 2024. Antibacterial activities of functional groups on the benzene rings in nucleic acid nanocarriers. Mater Today Chem 38: 102106. DOI: 10.1016/j.mtchem.2024.102106.

Yang R, Hou E, Cheng W, Yan X, Zhang T, Li S, Yao H, Liu J, Guo Y. 2022. Membrane-targeting neolignan-antimicrobial peptide mimic conjugates to combat Methicillin-Resistant *Staphylococcus aureus* (MRSA) infections. J Med Chem 65 (24): 16879-16892. DOI: 10.1021/acs.jmedchem.2c01674.

Yeo JD, Shahidi F. 2019. Revisiting DPPH (2,2-diphenyl-1-picrylhydrazyl) assay as a useful tool in antioxidant evaluation: A new IC100 concept to address its limitations. J Food Bioact 7 (21): 36-42. DOI: 10.31665/jfb.2019.7196.

Zakaria ZA, Kamsani NE, Azizah R, Sulistyorini L. 2022. Anticarcinogenic activity of methanol extract of *Melastoma malabathricum* leaves is attributed to the presence of phenolic compounds and the activation of endogenous antioxidant system. Bol Latinoam Caribe Plantas Med Aromat 21 (1): 66-80. DOI: 10.37360/blacpma.22.21.1.04.